Electron distribution function in a low-pressure inductively coupled plasma

V. I. Kolobov and W. N. G. Hitchon
Engineering Research Center for Plasma-Aided Manufacturing, University of Wisconsin–Madison, Madison, Wisconsin 53706
(Received 17 November 1994)

A method is presented for solution of the spatially inhomogeneous Boltzmann equation in the two-term approximation for low-pressure inductively coupled plasmas (ICP). The total electron energy $\varepsilon = w - e\phi$ (the sum of kinetic energy w and potential energy $e\phi$ in an electrostatic field) is used as an independent variable in the kinetic equation. Two energy ranges are distinguished. In the elastic energy range $w < \varepsilon^*$, where ε^* is the first excitation energy, the problem is effectively reduced to one variable (total electron energy) by performing an appropriate spatial average. The electron distribution function (EDF) in this energy range is a function solely of ε and does not depend explicitly on the coordinates. In the inelastic energy range, the kinetic equation in the variables (r, z, ε) (two spatial coordinates and the total energy) is solved for trapped and free electrons in a cylindrically symmetric ICP with a given spatial distribution of electric fields. The EDF and the spatial distributions of the electron current density and the ionization rate are calculated as functions of pressure, plasma density, and the profile of the electrostatic field. Explanations of some available experimental observations are given.

PACS number(s): 52.25.Dg, 52.50.Dg, 52.65.−y, 52.80.−s

I. INTRODUCTION

Recent demands in plasma processing of materials have resulted in the introduction of a new generation of plasma sources operated at low pressures 1 – 100 mTorr [1]. Modeling of these sources plays an important role in understanding the basic physical properties of the plasma and aids source design. For these low pressures, the main difficulties in discharge modeling arise from the necessity of rigorous kinetic treatment of electrons in spatially inhomogeneous plasmas in the presence of complicated electromagnetic fields. Since the electron energy relaxation length typically exceeds the source dimensions, the spatial nonlocalness of the electron spectrum is of vital importance. The spatial displacement of electrons occurs faster than their energy relaxation, thus the electron spectrum is governed by discharge properties in the whole volume, not just local characteristics. One striking nonlocal effect manifests itself in the spatial displacement of the ionization rate with respect to the electric power deposition. The hydrodynamic approach, which treats the electron gas as a fluid characterized by density, velocity, and mean energy, can give only a rather crude description of phenomena in low-pressure plasma sources.

One such "novel" plasma source which is increasingly being used in semiconductor manufacturing and other applications is an inductively coupled plasma (ICP). The ICP is sustained by an inductive RF electric field from a coil which results in electron heating. A planar coil configuration was developed to satisfy manufacturer's needs of plasma uniformity in a large volume [2]. The intrinsically two-dimensional character of ICP with a planar coil makes ICP modeling a rather complicated problem. Straightforward numerical simulation using Monte Carlo treatment of electrons is a computationally very demanding task [3]. Comparatively fast yet effective kinetic modeling of ICP has recently been demonstrated by Kortshagen and Tsendin [4], who self-consistently calculated the electron distribution function (EDF) and electric fields in the plasma. The model of Ref. [4], however, leaves out important physics since it is assumed that all electrons are trapped in the plasma by a static space-charge electric field. Calculation of the wall potential and kinetic treatment of free electrons which escape to the walls are necessary to explain the experimentally observed behavior of the light emission [5] and plasma uniformity as a function of gas pressure, coil design and chamber geometry.

One can take advantage of low operating pressures to simplify the treatment of nonlocal electron kinetics in the transition region between having no collisions and many collisions. In a weakly ionized low-pressure ICP, electron collisions with neutrals dominate over collisions between the charged particles. Even if the electron gas is collision dominated, it is the electron momentum which undergoes a substantial change in every collision with neutrals, not the electron energy. This is due to the large mass difference between the colliding partners. Thus, the energy relaxation length of the electrons greatly exceeds the momentum relaxation length. The dimensions of the discharge chamber are typically less than or comparable to the energy relaxation length. The so-called nonlocal approach, which was originated by Bernstein and Holstein [6] and Tsendin [7], is appropriate for these conditions. The key idea of this approach consists of using the total electron energy (kinetic plus potential in the static space-charge field) as the independent variable in the Boltzmann equation. This idea proved to be insightful and effective in application to various gas discharge problems [8–11] and has recently been applied to ICP

modeling in Refs. [4], [5], and [12]. For trapped electrons (which represent the vast majority of electrons in ICP) a further simplification can be achieved. Regardless of the multidimensional character of a discharge, an appropriate spatial averaging of the Boltzmann equation reduces the number of variables in the problem to only one (total energy). The experimental data [5,13] convincingly demonstrate that for the majority of electrons the EDF in a typical ICP is a function of total electron energy only and does not depend explicitly on the coordinates. Nevertheless, the spatial information is retained in the EDF calculated from the spatially averaged kinetic equation. This is revealed when the EDF is expressed in terms of the kinetic energy.

A relatively small fraction of electrons in an ICP cannot be treated using the spatially averaged kinetic equation. These are (i) free electrons which are capable of escaping to the chamber walls and (ii) fast electrons having an energy relaxation length less than the discharge dimensions. While these electrons give small contributions to the plasma density, they determine such important discharge characteristics as electron direct current density and the ionization rate. A rigorous treatment of these electrons is therefore just as important in ICP modeling as the description of slow electrons, which represent the vast majority of the ensemble.

The present paper is devoted to the kinetic treatment of electrons in ICP. We divide the electrons into different groups by total energy and demonstrate an effective method for numerical solution of the nonlocal Boltzmann equation in different energy ranges. We use the spatially averaged kinetic equation for slow electrons in the elastic energy range and solve the spatially inhomogeneous Boltzmann equation in the inelastic energy range (the EDF tail). We calculate the EDF, the ionization rate, and the electron fluxes in an ICP and compare our results with some available experimental data. In particular, we explain the experimentally observed dependence of the spatial distribution of light emission on the gas pressure [5].

II. ELECTRON BOLTZMANN EQUATION FOR ICP

We consider an ICP driven by an inductive electric field from a spiral coil placed on the dielectric roof of a squat cylinder of height L and radius R with metallic walls and bottom (Fig. 1). The azimuthal component of the RF inductive field E_θ (Fig. 1) is responsible for electron heating. The electrons and ions created by electron impact tend to diffuse out of the plasma, and, since electrons are faster, a positive space-charge excess develops in the volume. A space-charge field is built up which assists the ion current and retards the electron current. At high charge densities, when the electron Debye length is small compared to the discharge dimensions, a weak ambipolar space-charge field in the plasma gives rise to a combination of diffusive and mobility flow of charged particles. In the ambipolar regime, the electron and ion currents in the plasma are equal. In addition to the ambipolar field in the plasma, a potential drop in the sheath near the walls is set up to trap the majority of the electrons

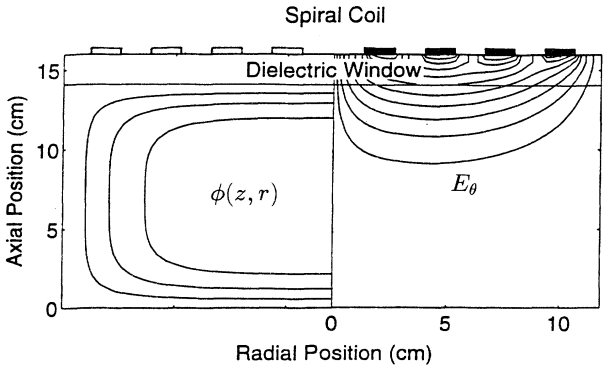

FIG. 1. Schematic of the discharge. The contour lines on the right show the levels of the calculated azimuthal RF field E_θ for an argon pressure $p = 30$ mTorr and a plasma density on axis of $n{=}10^{10}$ cm^{-3}. The contour lines on the left are equipotential lines of the electrostatic field E_s. These lines also indicate the discharge cross sections accessible to electrons with different total energies ε.

and assure the balance of total electron and ion currents to the walls. In a steady state, each electron must have, on average, one ionizing collision in the plasma before escaping. As the space-charge field reduces the electron escape rate it also reduces the required ionization rate. If the ionizing collision frequency is less than the elastic collision frequency, an electron undergoes many elastic collisions in the discharge volume before it escapes to the wall. Owing to the substantial change of electron momentum in an elastic collision, an almost isotropic EDF is formed for the majority of electrons regardless of the ratio of the electron mean free path to the discharge dimensions.

We assume that the total electric field has the form $\mathbf{E} = \mathbf{E}_s + \mathbf{E}_\theta \exp(i\omega t)$, where $\mathbf{E}_s$ is the DC space-charge field with potential $\phi(\mathbf{r})$ and E_θ is the azimuthal component of the RF inductive field (Fig. 1) with ω being its angular frequency. The shape of E_θ is determined by the coil design, by the influence of induced currents on the metallic sides of the chamber and by the plasma shielding. The equipotential lines of the field E_s are shown schematically in Fig. 1. In the general case, analysis of the electron spectrum which is formed in a bounded plasma with such a configuration of electric fields in the presence of different types of collisions is a rather complicated task. For a weakly ionized ICP, electron collisions with neutrals dominate over collisions between the charged particles. Specific features of the electron kinetics depend on the relation between the electron mean free path for momentum transfer, λ, and the characteristic discharge dimensions, L and R, as well as on the relation of the collision frequency to the RF field frequency ω.

We will consider primarily the collisional case when the electron mean free path λ is much smaller than both the dimensions of the chamber and the characteristic spatial scale of the RF field decay δ_s. It is supposed that the RF field strength is such that the oscillation amplitude of the

electron motion under the action of this field is small as compared to L, and the energy gained during the field period is smaller than characteristic energy of electrons. For most gases the transport frequency ν exceeds the total inelastic collision frequency ν^* at energies near the first electron excitation level ε^*, and the conventional two-term approximation for the EDF is applicable for all electron energies typical for ICP:

$$f(\mathbf{v},z,r,t) = f_0(v,z,r,t) + (\mathbf{v}/v)\cdot\mathbf{f}_1(v,z,r,t). \quad (1)$$

The EDF components are functions of the electron speed v, the spatial coordinates z and r, and time t. When expansion (1) is substituted into the Boltzmann equation where the magnetic field is neglected, and each term is expanded in spherical harmonics, one obtains [14,15]

$$\frac{\partial f_0}{\partial t} + \frac{v}{3}\nabla_r\cdot\mathbf{f}_1 + \frac{e}{3mv^2}\frac{\partial}{\partial v}(v^2\mathbf{E}\cdot\mathbf{f}_1) = C(f_0), \quad (2)$$

$$\frac{\partial \mathbf{f}_1}{\partial t} + v\nabla_r f_0 + \frac{e\mathbf{E}}{m}\frac{\partial f_0}{\partial v} = -\nu\mathbf{f}_1. \quad (3)$$

The collision term $C(f_0)$ depends only on the isotropic part f_0. Electron collisions with neutrals in the considered energy range can be unambigously divided into quasielastic and inelastic. Quasielastic collisions include those with small energy loss compared to the electron energy, i.e., elastic collisions and excitation of molecular vibrations and rotations. They are described by the Fokker-Planck collision integral and characterized by the parameter $\delta \ll 1$ which is the average fraction of the energy lost in a single collision. For atomic gases, $\delta = 2m/M \ll 1$, where M is the atom mass. For typical electron energies in ICP, inelastic collisions lead to an energy loss comparable to the electron energy, e.g., in excitation of electron levels and ionization of neutrals. They are represented by an absorbing term in the kinetic equation (see below) and characterized by the frequency $\nu^*(v)$. The electron-electron collision operator can be written in the Fokker-Planck form with characteristic frequency

$$\nu_{ee} = \frac{4\pi e^4 n\Lambda}{m^2 v^3}, \quad (4)$$

where n is the electron density and Λ is the Coulomb logarithm.

For typical pressures, the energy relaxation length in elastic collisions $\lambda_T = \lambda\delta^{-1/2} \gg \lambda$ greatly exceeds the discharge dimensions. For typical plasma densities, $\nu_{ee} \ll \nu$ for the majority of electrons. The EDF relaxation length due to ee collisions is given by $\lambda_{ee} = \lambda(\nu/\nu_{ee})^{1/2}$. Since an electron performs a random walk with the step λ, the length λ_{ee} corresponds to the electron displacement during the time ν_{ee}^{-1} between subsequent ee collisions. When the EDF relaxation length exceeds the discharge dimensions, it is useful to include the influence of the static field on the electron kinetics using the total energy of the electrons $\varepsilon = w - e\phi$, where w is their kinetic energy, as an independent variable. Since the change of the total energy due to electron heating by the RF field and energy transfer in collisions are slow compared to the time scale of the spatial displacement of electrons, the total energy ε is approximately an integral of the electron motion.

The time scale of f_0 relaxation is determined by the collision integral $C(f_0)$. Since $\nu^* \ll \nu, \delta\nu \ll \nu$, f_0 relaxation is much slower than momentum relaxation which occurs with the time scale ν^{-1}. In the presence of the RF inductive field of the frequency $\omega \gg \nu^*$, and the static space-charge field, the isotropic component f_0 is modulated only slightly and can be assumed constant to a first approximation. The anisotropic part $\mathbf{f}_1$ breaks into oscillatory and steady-state parts:

$$\mathbf{f}_1 = \mathbf{f}_1^0(v,z,r) + \mathbf{f}_1^1(v,z,r)\exp(i\omega t). \quad (5)$$

Bearing in mind the above assumptions and using the total energy ε as an independent variable, one can rewrite Eqs. (2) and (3) in the form

$$\nabla_r\cdot(vD_r\nabla_r f_0) + \frac{\partial}{\partial\varepsilon}vD_E\frac{\partial f_0}{\partial\varepsilon} = vC(f_0), \quad (6)$$

$$\mathbf{f}_1^0 = -\frac{v}{\nu}\nabla_r f_0, \quad (7)$$

$$\mathbf{f}_1^1 = -\frac{ve\mathbf{E}_\theta}{\nu + i\omega}\frac{\partial f_0}{\partial\varepsilon}. \quad (8)$$

Equation (6) is obtained by substituting $\mathbf{f}_1^0(z,r,\varepsilon)$ and $\mathbf{f}_1^1(z,r,\varepsilon)$ from (7) and (8) and averaging over the oscillation period. In this approximation $\mathbf{f}_1^1$ is determined by the local value of the RF field. Thus we neglect the spatial dispersion of the electron conductivity and the collisionless electron heating [16–18]. The left-hand side of Eq. (6) describes the electron diffusion in configuration space and in energy. The diffusion coefficient $D_r(z,r,\varepsilon) = v\lambda/3$ and the diffusion coefficient in energy

$$D_E(z,r,\varepsilon) = \frac{(eE_\theta(z,r)\lambda)^2\nu^3}{6(\nu^2+\omega^2)} = \frac{1}{3}(eE_{\text{eff}}\lambda)^2\nu \quad (9)$$

are functions of the coordinates and the total electron energy. According to Eq. (6), the time-averaged energy gain from the RF field corresponds to diffusion in ε. The diffusion coefficient in energy is proportional to the square of the effective field $E_{\text{eff}} = (E_\theta/\sqrt{2})[1+(\omega/\nu)^2]^{1/2}$ which rapidly vanishes with increasing distances from the coil. The heating is therefore spatially inhomogeneous and occurs mainly in the vicinity of the coil.

Let the maximal value of $\phi(z,r)$ in the plasma correspond to $\phi = 0$. The wall potential ϕ_w is set up to ensure the integral balance of ionization and electron escape to the walls. Since the characteristic time for electron spatial diffusion is small compared to the time between subsequent ionizing collisions, $-e\phi_w$ must exceed the lowest excitation potential of atoms ε^* (or the ionization potential, if direct ionization prevails) [8]. Using the total energy ε as the independent variable, we distinguish two energy ranges. The elastic energy range corresponds to $\varepsilon < \varepsilon^*$. The electrons in this energy range are trapped in the potential well. The only mechanisms for their energy relaxation are elastic collisions and electron-electron in-

teractions. The electrons in the inelastic energy range, $\varepsilon > \varepsilon^*$, can be subdivided into two groups: trapped (with $\varepsilon < -e\phi_w$) and free (with $\varepsilon > -e\phi_w$). We consider below specific features of electron kinetics in the elastic and inelastic energy ranges.

III. INELASTIC ENERGY RANGE

Practically the whole discharge area is accessible to electrons in the inelastic energy range. The EDF tail (at $\varepsilon > \varepsilon^*$) in the collisional case comprises a small fraction of the total number of electrons and exponentially decreases with ε [12]. Consequently, in inelastic collisions most electrons lose almost all their energy. The source of electrons can be neglected in the inelastic energy range. Since the electron-electron collision frequency decreases rapidly as the electron velocity increases, the electron-electron interactions do not influence the EDF in the inelastic energy range. Taking into account only important terms, the kinetic equation (6) in the inelastic energy range can be written in the form

$$\nabla_r \cdot (vD_r \nabla_r f_0) + \frac{\partial}{\partial \varepsilon} v D_E \frac{\partial f_0}{\partial \varepsilon} = v\nu^*(w)\Theta(\varepsilon - \varepsilon^* - e\phi(r,z)) f_0, \quad (10)$$

where $\nu^*(w)$ is the total frequency of inelastic collisions. The left-hand side of (10) describes the particle diffusion in space and in energy with coordinate and energy-dependent diffusion coefficients. The right-hand side represents the particle absorption. The step function $\Theta(x)$ emphasizes that the "absorbing" region in the (z,r) space (the area where inelastic collisions occur) occupies only that part of the discharge volume where the electrons with total energy ε have kinetic energy w sufficient for excitation. The energy relaxation length of fast electrons (with $w > \varepsilon^*$) from Eq. (10) is given by $\lambda^* \approx \lambda(\nu/\nu^*)^{1/2} \gg \lambda$. This length corresponds to electron displacement during the time $1/\nu^*$. Since electrons undergo a random walk with step size λ, the length λ^* is a net distance an electron travels before an inelastic collision occurs. This length differs evidently from the mean free path with respect to inelastic collisions, v/ν^*. Since typically $\lambda^* \ll \lambda_T$, the requirement of the EDF nonlocality is more stringent in the inelastic energy range. When $\lambda^* \ll L \ll \lambda_T$ the EDF in the elastic energy range ($\varepsilon < \varepsilon^*$) is nonlocal while the EDF in the inelastic energy range is almost local. In this case, a strong depletion of the EDF tail is expected in the "absorbing" region in the (z,r) space where inelastic collisions occur.

Neglecting the sheath thickness, the boundary conditions for both trapped and free electrons can be specified at the chamber walls. The boundary condition for trapped electrons corresponds to their reflection by the potential well:

$$\frac{\partial f_0}{\partial \eta} = 0, \quad (11)$$

where η denotes the direction normal to the walls. Free electrons (with total energy $\varepsilon > -e\phi_w$) are capable of escaping from the discharge. The isotropy of the EDF is disrupted within a length λ of the walls (because of the absence of an inverse flux). To escape from the discharge an electron with $\varepsilon > -e\phi_w$ must move toward the wall, i.e., after the last scattering its velocity must lie in a loss cone. The loss cone is determined by the condition that electron kinetic energy associated with motion in the direction normal to the wall exceeds the potential drop in the sheath $e\Delta\phi$. A boundary condition at $\varepsilon > -e\phi_w$ can be obtained by imposing equality of the normal component of the electron diffusive flux and the electron loss to the wall [19]:

$$-D_r \frac{\partial f_0}{\partial \eta} = v f_0 \frac{\Omega}{4\pi}, \quad (12)$$

where $\frac{\partial f_0}{\partial \eta}$ is the derivative normal to the wall. The fraction $\Omega/2\pi$ represents the fraction of the thermal flux lost. The solid angle Ω of the loss cone is given by

$$\Omega = 2\pi \left(1 - \sqrt{\frac{e\Delta\phi}{\varepsilon + e\phi_{\rm sh}}}\right). \quad (13)$$

Electrons having kinetic energy $w = \varepsilon + e\phi_{\rm sh}$ near the wall and managing to get into the loss cone after the last scattering can overcome the potential drop $\Delta\phi$ and reach the absorbing wall.

IV. ELASTIC ENERGY RANGE

Energy loss in elastic collisions with neutrals and electron-electron interactions are the only mechanisms for EDF relaxation in the elastic energy range $\varepsilon < \varepsilon^*$. Under nonlocal conditions the corresponding relaxation lengths exceed the chamber dimensions, and the slow electrons bounce in the potential well with (almost) constant total energy. The surface $\varepsilon = -e\phi(z,r)$ bounds the area accessible to electrons with energy ε. Since the spatial displacement of electron occurs rapidly compared to the total energy change due to collisions and heating, a spatial averaging of Eq. (6) over the accessible area can be performed [10,12]. The idea of spatial averaging, originated by Bernstein and Holstein [4] and Tsendin [5], is analogous to that of time-averaging used above to derive Eq. (6). In the case of a time-dependent field the electron energy gain averaged over the field period is governed by an effective electric field $E_{\rm eff}$. In a spatially inhomogeneous case, due to rapid electron diffusion, the whole available discharge cross section contributes to the EDF formation. This means that the heating rate is determined by a spatially averaged field E_θ rather than its local value, the effective energy transfer in ee collisions is determined by the whole plasma density profile in the discharge volume, etc. This nonlocal case can therefore be considered as the opposite limit to the local case where the EDF is governed by local parameters of the plasma.

According to the Bernstein-Holstein-Tsendin (BHT) method, the EDF of trapped electrons under nonlocal conditions can be expressed in the form

$$f_0(r,z,\varepsilon) = f_0^{(0)}(\varepsilon) + f_0^{(1)}(r,z,\varepsilon) \quad (14)$$

where the principal part $f_0^{(0)}(\varepsilon)$ is a function of the total

energy only, and $f_0^{(1)}(r,z,\varepsilon)$ is a small correction. The EDF $f_0^{(0)}(\varepsilon)$ can be calculated from a spatially averaged Boltzmann equation. Integrating Eq. (6) over the volume accessible to electrons with total energy ε, one obtains

$$\frac{d}{d\varepsilon}\left\{\left(\langle vD_E\rangle + \langle vD_{ee}\rangle\right)\frac{df_0^{(0)}}{d\varepsilon} + \left(\langle vV_{ee}\rangle + \langle vV_{eN}\rangle\right)f_0^{(0)}\right\} = \langle vI\rangle. \quad (15)$$

The angular brackets $\langle\,\rangle$ designate integration over the accessible volume of the discharge. For a quantity $G(r,z,w)$, due to axial symmetry

$$\langle G\rangle = 2\pi\int_{S(\varepsilon)} G(\varepsilon + e\phi(x))r\,dr\,dz, \quad (16)$$

where $S(\varepsilon)$ is the available area bounded by the curve $\varepsilon = -e\phi(z,r)$. The shape of the EDF is governed by the balance between the electron energy diffusion caused by heating and ee collisions and dynamical friction caused by energy loss in elastic collisions ($V_{eN} = w\delta\nu$) and ee interactions; I is the source of slow electrons. The electron-electron collision integral is written in the Fokker-Planck form with diffusion coefficient $D_{ee} = 2mw\nu_{ee}A_1$ and dynamical friction coefficient $V_{ee} = 2w\nu_{ee}A_2$. Functions $A_1(f_0)$ and $A_2(f_0)$ are given by

$$A_1 = \frac{2\pi}{3n}\left(\frac{2}{m}\right)^{5/2}\left\{\int_0^w w^{3/2}f_0\,dw + w^{3/2}\int_w^\infty f_0\,dw\right\}, \quad (17)$$

$$A_2 = \frac{2\pi}{n}\left(\frac{2}{m}\right)^{3/2}\int_0^w w^{1/2}f_0\,dw, \quad (18)$$

where $w(\varepsilon,z,r)$ is the kinetic energy. For $w\to\infty$, $A_1 \to T_e/m$ and $A_2 \to 1$, where T_e is the electron temperature. The electron density is given by

$$n(z,r) = 2\pi\left(\frac{2}{m}\right)^{3/2}\int_{-e\phi}^\infty f_0(\varepsilon)\sqrt{\varepsilon + e\phi}\,d\varepsilon. \quad (19)$$

Dividing Eq. (15) by $\langle v\rangle$ one obtains

$$\frac{1}{\langle v\rangle}\frac{d}{d\varepsilon}\langle v\rangle\left\{\left(\mathcal{D}_E + \mathcal{D}_{ee}\right)\frac{df_0^{(0)}}{d\varepsilon} + \left(\mathcal{V}_{ee} + \mathcal{V}_{eN}\right)f_0^{(0)}\right\} = \mathcal{I}, \quad (20)$$

where the quantities $\mathcal{D}_E, \mathcal{D}_{ee}, \mathcal{V}_{ee}, \mathcal{V}_{eN}$, and $\mathcal{I}$ designate the spatially averaged values, e.g., $\mathcal{D}_E = \langle vD_E\rangle/\langle v\rangle$, etc. The quantity $\langle v\rangle$ describes the change of the phase space volume with change of ε. The procedure of spatial averaging reduces the problem of the EDF calculation to the solution of the ordinary differential equation (20). The physical meaning of spatial average is straightforward. Due to rapid electron diffusion, the whole available discharge cross section contributes to the formation of the EDF. Though the EDF in (20) does not explicitly depend on the coordinates, the spatial information is retained implicitly, as is revealed when the EDF is expressed in the kinetic energy domain. The EDF versus kinetic energy at a given position can be found from the relation

$$f_0^{(0)}(w,r,z) = f_0^{(0)}(\varepsilon = w - e\phi(r,z)) \quad (21)$$

which can be treated as a generalization of the Boltzmann relation for a non-Maxwelliam EDF. Expression (21) splits up into a product of two factors, one depending only on the coordinates and the other on the kinetic energy, only in the case of a Maxwellian EDF $f_0(\varepsilon)$. In this case, Eq. (21) corresponds to a Maxwell-Boltzmann distribution, and the electron density from Eq. (19) is given by the conventional formula $n_e \sim \exp(e\phi/T_e)$.

The EDF $f_0^{(0)}(\varepsilon)$ corresponds to exact compensation of electron drift and diffusion fluxes for each ε. However, the diffusion and drift *energy* fluxes are only compensated on average over the discharge cross sections. The small correction term $f_0^{(1)}$ which describes the electron flux in configuration space can be obtained from Eq. (6) as described in Ref. [7].

The solution of the spatially averaged Boltzmann equation (20) should be matched to the solution of the full equation (6) at energies slightly below the excitation potential ε^*. In the case $\lambda^* < L$ the EDF may depend explicitly on the coordinates even in the elastic energy range in the vicinity of ε^*. For low pressures when $\lambda^* \gg L$ the averaging is applicable for trapped fast electrons as well. In this case the EDF does not depend explicitly on the coordinates up to energies near the wall potential.

V. RESULTS

Though spatially resolved measurements of EDF's in ICP are available [5,13], the purpose of the present study was to examine the influence of different parameters on the EDF shape rather than perform detailed calculations for specific experimental conditions. Thus, the data for necessary collision cross sections were assumed to have a simple analytic form [10]. The electrostatic potential profile $\phi(z,r)$ in the plasma was chosen in the form

$$\phi(z,r) = \phi_{\rm sh}\left[1 - \left(\frac{2z}{L} - 1\right)^\kappa\right]\left[1 - \left(\frac{r}{R}\right)^\kappa\right] - \phi_{\rm sh}, \quad (22)$$

where $\phi_{\rm sh}$ is the potential at the plasma-sheath boundary. The thickness of the sheath was neglected and the wall potential ϕ_w was defined to guarantee the balance of electron production and escape [5]. The azimuthal component of the RF electric field E_θ was calculated for given coil current and plasma density as in Ref. [4]. We have calculated the EDF, the light emission spatial distribution and electron flux for different argon pressures, plasma densities, and profiles of the potential in the plasma.

The EDF body was calculated from Eq. (20), and matched to the solution of (10) for the EDF tail at

$\varepsilon = 0.8\varepsilon^*$. The discretized partial differential equation (10) was solved using Newton's method. For each Newton iteration, a relevant linear matrix equation was solved using Gaussian elimination. We used a software package [20] especially designed for large-scale computational problems in applied physics.

Figure 2 illustrates the κ dependence of $\mathcal{D}_E$ and the EDF. For a rectangular potential well ($\kappa \to \infty$) the entire cross section of the discharge chamber is accessible to electrons. The EDF shape is determined by a spatially averaged value of the RF field [according to Eq. (20)]. For a rectangular potential well, the quantity $\mathcal{D}_E$ decreases with ε only due to the $\nu(v)$ dependence. As in a spatially homogeneous case, concave and convex EDF's in the semilogarithmic plot versus ε can be obtained for a Ramsauer gas for different ratios of ω/ν. For finite κ, an additional decrease of $\mathcal{D}_E$ with ε is caused by the strong nonuniformity of the heating field. The decrease in skin layer thickness results in cooling of the slowest electrons. These electrons cannot overcome the ambipolar potential barrier and thus cannot reach the region of high E_θ where the heating occurs. Due to both these circumstances, the averaged energy diffusion coefficient $\mathcal{D}_E$ in argon vanishes at low electron energies [Fig. 2(a)]. The electron-electron interactions are the only mechanism of energy exchange for the slowest electrons. In ICP, they prevent formation of a large peak at low energies such as is observed in capacitively coupled plasmas, where the plasma density is usually smaller [21]. The more the energetic electrons penetrate into the RF field region, the larger is $\mathcal{D}_E$. Consequently the EDF slope in this energy range diminishes with increasing of ε [Fig. 2(b)].

The solution of the full kinetic equation, Eq. (10), has been performed in the inelastic energy range. The calculated EDF's are shown in Fig. 3 for two different pressures at various spatial positions as functions of the total electron energy. For the high-pressure case ($\lambda^* < L$), depletion of the EDF tail is observed in the region of the highest dc potential (where inelastic collisions occur). In the low-pressure case, the EDF tail depends on the position for free electrons only. For this case, an important nonlocal effect appears in the spatial separation of electron heating and ionization, similar to that in capacitive RF discharges [21]. Though the electron heating occurs in the region of high RF field, a maximum of the ionization is produced near the maximum of the electrostatic potential $\phi(z,r)$ where the RF field is absent.

Figure 4 shows the calculated spatial distribution of the excitation rate. It allows us to explain the difference between the experimentally observed shapes of the light emission for different pressures [5]. With the pressure decrease the maximum of the light emission moves from off axis where the heating takes place to the discharge axis where the maximum of the electrostatic potential occurs (see Fig. 4). Beyond the heating region in the vicinity

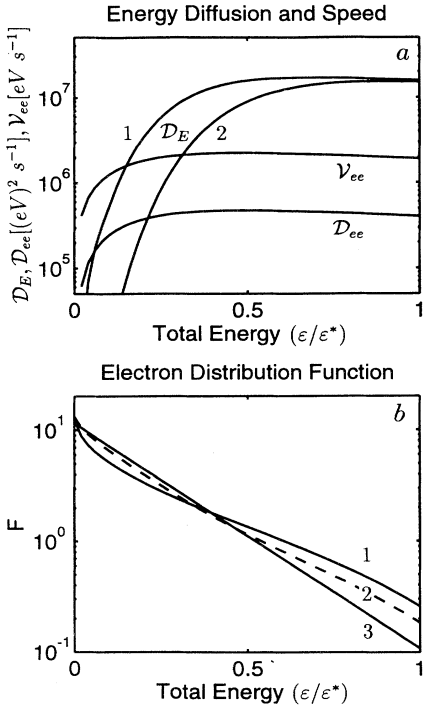

FIG. 2. (a) Space-averaged diffusion coefficients in energy $\mathcal{D}_E(\varepsilon)$ and $\mathcal{D}_{ee}(\varepsilon)$ and velocity $\mathcal{V}_{ee}(\varepsilon)$ for $\kappa = 4$ (curve 1) and $\kappa = 2$ (curve 2), plasma density $n = 10^{11}$ cm^{-3}. (b) The dimensionless EDF $F = \frac{2\pi}{n}(\frac{2\varepsilon^*}{m})^{3/2} f_0$ in the elastic energy range for different shapes of the electrostatic potential, Eq. (14), and plasma density n: 1, κ=2, $n = 5\times10^9$ cm^{-3}; 2, κ=4; $n = 5\times10^9$ cm^{-3}; 3, κ=2, $n = 10^{11}$ cm^{-3}. $p = 30$ mTorr, $-e\phi_{sh} = \varepsilon^*$.

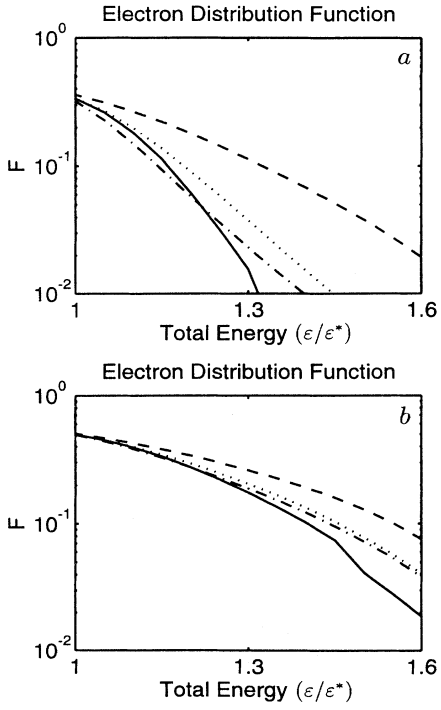

FIG. 3. The dimensionless EDF $F = \frac{2\pi}{n}(\frac{2\varepsilon^*}{m})^{3/2} f_0$ in the inelastic energy range for (a) $p = 30$ mTorr, $-e\phi_w$=1.3 ε^* and (b) p= 10 mTorr, $-e\phi_w$=1.5 ε^*. Solid line, $r = 6$ cm, $z = 1$ cm; dotted line, $r = 6$ cm, $z = 7$ cm; dashed line, $r = 6$ cm, $z = 13$ cm; dash-dot line, $r = 0$ cm, $z = 7$ cm.

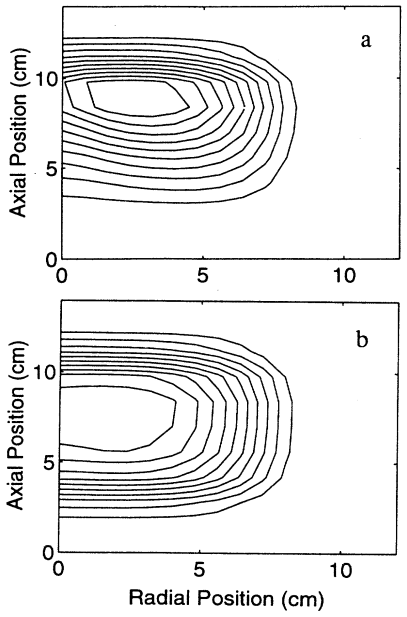

FIG. 4. Contours of the ionization rate for two pressures: (a) $p = 30$ mTorr, (b) 10 mTorr. $n = 10^{11}$ cm^{-3}, $k = 4$, wall potential $-e\phi_w = 1.5\varepsilon^*$.

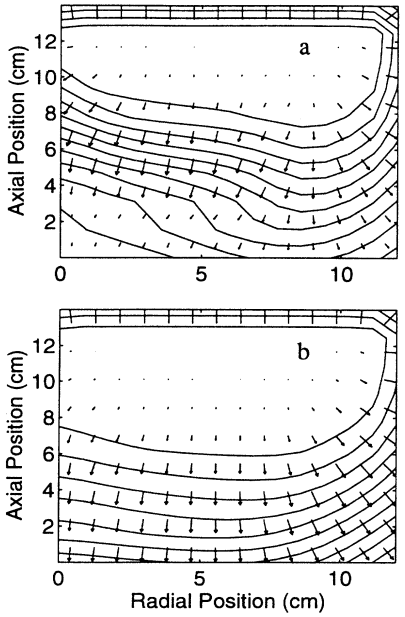

FIG. 5. Spatial distribution of the electron dc current density for (a) $p = 30$ mTorr, (b) 10 mTorr. The arrows show the direction and the magnitude of the dc current density, the solid lines show the EDF levels for electrons with a fixed total energy $\varepsilon = 1.3\varepsilon^*$.

of the coil, the electrons diffuse with conservation of the total energy and have the highest kinetic energy in the region of the highest electrostatic potential. The maximum of the light emission is observed here at low pressures. This maximum moves off axis when the electron energy relaxation length in inelastic collisions becomes less than the discharge dimensions and the fast electrons suffer from inelastic collisions before reaching the region of the highest potential.

The electron current density in ICP has both direct j_s and alternating j_c components. They are determined by the components $\mathbf{f}_1^0$ and $\mathbf{f}_1^1$ of the EDF. These are in turn found to be derivatives of f_0. Thus, from Eqs. (7) and (8) one obtains

$$\mathbf{j}_c(z,r) = -\frac{4\pi e^2 \mathbf{E}_\theta}{3m} \int_{-e\phi(r,z)}^{\infty} \frac{v^3}{\nu + i\omega} \frac{\partial f_0}{\partial \varepsilon} d\varepsilon, \tag{23}$$

$$\mathbf{j}_s(z,r) = -\frac{4\pi e}{3m} \int_{-e\phi(r,z)}^{\infty} \frac{v^3}{\nu} (\nabla f_0)\, d\varepsilon. \tag{24}$$

The calculated current density $\mathbf{j}_s$ is shown in Fig. 5 for two pressures. The arrows indicate the direction and the amplitude of $\mathbf{j}_s$. The contour lines in Fig. 5 indicate the EDF levels at fixed total energy. The highest density of electrons in the inelastic energy range is observed in the vicinity of the coil where the energy diffusion coefficient $D_E(z,r,\varepsilon)$ has a maximum with respect to the coordinates. It is worth emphasizing that the maximum value of the total electron density for these conditions is reached on axis.

VI. DISCUSSION

The model described here is applicable in a specific range of discharge conditions. The assumptions described in Sec. II require that the pressure be sufficiently low to assure the electron energy relaxation length in the elastic energy range be larger than the chamber dimensions. On the other hand the pressure must be comparatively high to assure the neglect of collisionless electron heating. The plasma density must be low enough to prevent the localization of the EDF due to electron-electron interactions.

Electron kinetics under nonlocal conditions differ considerably from local hydrodynamic behavior. Some striking examples can be listed. Both dc and ac densities j_c and j_s given by Eqs. (23) and (24) differ from the classical hydrodynamic expressions. Since in the collisional case considered here the spatial dispersion of the electron conductivity was neglected, the ac density j_c is proportional to the local value of the RF electric field. However, j_c is not proportional to the local electron density, as in the hydrodynamic case, but is determined by the plasma properties in the entire volume through the nonlocal EDF. As the pressure decreases, when collisionless electron heating comes into play, j_c begins to be governed by the entire RF field profile rather than a local field value.

The fluid approach divides the dc current density $\mathbf{j}_s$ into diffusion and drift parts:

$$\mathbf{j}_s = -eD_e \nabla n - e\mu_e n_e \mathbf{E}_s, \tag{25}$$

where the electron diffusion and mobility coefficients are integral characteristics of the electron spectrum. In the nonlocal case, these coefficients are functions of the coordinates. They cannot be calculated *a priori* without knowledge of the EDF. Since in the nonlocal case the electrons of different ε behave almost independently, they contribute in an entirely different fashion to such integral EDF quantities as density, mean velocity, and temperature. According to the BHT approach, the EDF of trapped electrons in the elastic energy range is only a function of total energy and does not depend explicitly on the coordinates. These electrons therefore give no contribution to dc density j_s while they are primarily responsible for the ac density j_c and the plasma density. The mechanism of electron diffusion in low-pressure bounded plasmas differs considerably from classical ambipolar diffusion. For trapped electrons, the (energy resolved) electron diffusion flux against the field E_s is exactly canceled by the mobility flux . The electron dc density j_s is transported only by free electrons and those electrons in the inelastic energy range whose EDF depends explicitly on the coordinates. It is worth emphasizing that the density of trapped electrons exceeds the density of untrapped electrons by orders of magnitude, but the contribution of slow electrons to the dc current is zero in this model. When the dc density is transported only by "free" diffusion of the untrapped electrons, it is in principle impossible to express j_s in terms of the total electron density and its derivatives [9]. Therefore, Eq. (25) is altogether misleading in this case and can result in substantial errors. Attempts to express the current density j_s in terms of other characteristics averaged over the entire EDF (e.g., electron temperature), or addition of the thermodiffusion term to Eq. (25), do not substantially improve its accuracy.

Since the EDF is a function of total electron energy, the mean kinetic energy of electrons is spatially uniform only for a Maxwellian EDF $f_0(\varepsilon)$. For a non-Maxwellian EDF [represented by a convex (concave) curve on a semilogarithmic plot of f_0 versus ε], the mean kinetic energy of the electrons decreases (increases) from the point of maximum potential towards the chamber walls [21].

The inequality $\nu^* < \nu$ assures the small anisotropy of the EDF for the majority of electrons even for the free-flight regime $\lambda > L$. In this regime, the trapped electrons perform many bounces in the well and pass the heating region many times before being heated enough to be lost to the wall. Collisionless electron heating in this regime may prevail over Ohmic heating. Equation (20) for the isotropic part of the EDF is expected to be applicable in this case if the energy diffusion coefficient is replaced in an appropriate manner. If the heating region occupies a small part of the discharge volume, the spatially averaged diffusion coefficient in energy, $\mathcal{D}_E(\varepsilon)$, can be expressed in terms of the energy $\Delta\varepsilon$ gained during one passage through the heating region and the bounce frequency $\Omega_b \sim v/L$ [22],

$$\mathcal{D}_E(\varepsilon) = \langle v(\Delta\varepsilon)^2\Omega_b\rangle/\langle v\rangle. \tag{26}$$

An electron gains net energy after (collisionlessly) traversing the heating region in a time short compared to the period of the field [22,23]. If the characteristic scale on which the RF field decreases is δ_s, an essentially collisionless heating occurs at $\omega\delta_s < v$. The influence of the RF magnetic field on the electron motion within the skin layer may be important [24]. For the case $\delta_s \ll \lambda \ll L$ the return of electrons into the skin layer is caused by scattering [23]; the collision frequency ν should be used instead of the bounce frequency for calculation of the energy diffusion coefficient (26). The EDF formation in the collisionless regime of electron heating will be treated in detail elsewhere.

The main conclusions of the present work are as follows. (i) The approximation of small anisotropy of the EDF is applicable for ICP in a wide range of gas pressures. (ii) Total energy is an appropriate variable for analysis of nonlocal electron kinetics. Using the total energy, two energy ranges can be separated. The EDF in the elastic energy range is a function solely of the total energy and does not depend explicitly on the coordinates. (iii) Contrary to the local approach, the nonlocal EDF in the elastic energy range depends on integral characteristics of the plasma (fields, collisions) rather than their local values. (iv) The EDF in the inelastic energy range depends crucially on the ratio of the fast electron energy relaxation length and the spatial scale of the discharge. Various spatial distributions of the light emission, the ionization rate, and the electron current may be observed as the gas pressure varies.

VII. SUMMARY

We have obtained a numerical solution of the nonlocal Boltzmann equation in the two-term approximation for inhomogeneous bounded plasmas in the presence of static and RF electric fields. We have presented a relatively simple approach to the kinetic treatment of electrons in a low-pressure ICP which offers considerable physical insight and is very efficient computationally. We used it to explain the spatial behavior of the EDF as well as the ionization rate and electron current. The EDF in the present model is not found self-consistently with the electric fields. Self-consistent ICP modeling is in progress where the proposed model of the electron kinetics is combined with a consistent solution of the ion continuity equation, Poisson's equation, and the Maxwell equations for the RF field.

ACKNOWLEDGMENTS

This work was supported in part by NSF under Grant No. ECD-8721545. We thank D.F. Beale for help with some of the numerical calculations.

[1] M.A. Lieberman and R.A. Gottscho, *Physics of Thin Films*, edited by M. Francombe and J. Vossen (Academic, New York, 1994), Vol. 18, pp. 1–119.
[2] J.H. Keller, J.C. Foster, and M.S. Barnes, J. Vac. Sci. Technol. A **11**, 2487 (1993).
[3] P.L.G. Ventzek, R.J. Hoekstra, and M.J. Kushner, J. Vac. Sci. Technol. B **12**, 461(1994).
[4] U. Kortshagen and L.D. Tsendin, Appl. Phys. Lett. **65**, 1355 (1994).
[5] V.I. Kolobov, D.F. Beale, L.J. Mahoney, and A.E. Wendt, Appl. Phys. Lett. **65**, 537 (1994).
[6] I.B. Bernstein and T. Holstein, Phys. Rev. **94**, 1475 (1954).
[7] L.D. Tsendin, Sov. Phys. JETP **39**, 805 (1974).
[8] L.D. Tsendin and Yu.B. Golubovsky, Sov. Phys. Tech. Phys. **22**, 1066 (1977).
[9] V.I. Kolobov and L.D. Tsendin, Phys. Rev. A **46**, 7837 (1992).
[10] I.D. Kaganovich and L.D. Tsendin, IEEE Trans. Plasma Sci. **20**, 66 (1992).
[11] U. Kortshagen, Phys. Rev. E **49**, 4369 (1994).
[12] D.F. Beale, W.N.G. Hitchon, V.I. Kolobov, and A.E. Wendt, Proceedings of the 47th Annual Gaseous Electronics Conference, October, 1994, Gaithersburg, Maryland [Bull. Am. Phys. Soc., Ser. II **39**, 1489 (1994)].
[13] U. Kortshagen, I. Pukropski, and M. Zethoff, Appl. Phys. **76**, 2048 (1994).
[14] V.E. Golant, A.P. Zhilinsky, I.E. Sakharov, and S.C. Brown, *Fundamentals of Plasma Physics* (Wiley, New York, 1980).
[15] I.P. Shkarofsky, T.W. Johnston, and M.P. Bachynsky, *The Particle Kinetics of Plasmas* (Addison-Wesley, Reading, MA, 1966).
[16] M.M. Turner, Phys. Rev. Lett. **71**, 1844 (1993).
[17] V.A. Godyak, R.B. Piejak, and B.M. Alexandrovich, Plasma Sources Sci. Technol. **3**, 169 (1994).
[18] V. Vahedi, G. DiPeso, M.A. Lieberman, T.D. Rognlien, and D. Hewett (unpublished).
[19] C. Busch and U. Kortshagen, Phys. Rev. E **51**, 280 (1995).
[20] K.M. Kramer and W.N.G. Hitchon, Comput. Phys. Commun. **85**, 167 (1995).
[21] V.A. Godyak and R.B. Piejak, Appl. Phys. Lett. **63**, 3137 (1993).
[22] C.E. Goedde, A.J. Lichtenberg, and M.A. Lieberman, J. Appl. Phys. **64**, 4375 (1988).
[23] V.V. Vas'kov, A.V. Gurevich, and Ya.S. Dimant, Sov. Phys. JETP **57**, 310 (1983).
[24] T.D. Rognlien, R.H. Cohen, G.J. DiPeso, V. Vahedi, and D.W. Hewett, Proceedings of the 47th Annual Gaseous Electronics Conference, October, 1994, Gaithersburg, Maryland [Bull. Am. Phys. Soc., Ser. II **39**, 1414 (1994)].